 Internaitonal Journal of Turbo and Jet-Engines 4, 131-138 (1987)

Flow Measurements in Two Cambered Vane Diffusers with Different Passage Widths

W. Stein and M. Rautenberg
University of Hannover, West Germany

Abstract

To investigate the influence of the vaneless space between impeller exit and the diffuser vanes, detailed flow measurements in two diffusers with the same vane geometry but different passage width are compared.

The three-dimensional character of the flow changes between impeller exit and the entry to the two dimensional vanes depending on the shape of the shroud. After initial measurements with a constant area vaneless space, the width of the vaned diffuser was later on reduced by 10%. The compressor maps show an increase in overall pressure rise and efficiency with the width reduction.

To get further details of the flow field, measurements of the static pressure distribution at hub and shroud have been performed at several operation points for both diffusers. At the same points the flow angle and total pressure distribution between hub and shroud upstream and downstream of the vanes have been measured with probes. The maximum efficiency of the narrow diffuser is nearly 2% higher than for the wide diffuser. The measurements give further details to explain these improvements.

Nomenclature

b	diffuser width, m
d	diameter, m
$\dot{m}$	mass flow, kg/s
n	shaft speed, rpm
p	pressure, bar
r	radius, m
T	diffuser pitch, m, temperature, K
Y	coordinate in circumferential direction, m
Z	blade number
z	axial coordinate, m
η	efficiency, %
κ	isentropic exponent
λ	d/d_2 diffuser diameter ratio
$\bar{\pi}$	p/p_k pressure ratio
τ	temperature ratio

Subscripts

0	reference conditions
2	impeller exit
4	diffuser inlet
6	diffuser outlet
K	stagnation condition in the equalizing chamber
s	isentropic
tot	stagnation

Introduction

In the design of centrifugal compressors it is necessary to get an optimum of efficiency, the correct design-mass-flow or pressure ratios by optimizing the impeller. However, the characteristic of the machine is also affected by the other aerodynamic components such as an inlet and outlet section, a scroll and a diffuser.

Some years ago a lot of attention was paid to the optimum design of vaneless diffusers because they achieve a good overall characteristic with little manufacturing effort. In the recent years more and more vaned diffusers were necessary to reach high efficiencies and high pressure ratios of a compressor stage. There are quite a lot of different

possible vane – or channeltypes of this component. A lot more parameters must be specified for the design of a vaned diffuser, and the performance prediction must be carried out more precisely to reach the design point as compared to the design of vaneless diffusers.

Therefore there is a large number of comparisons of different diffuser types in the literature. In most of these publications the performance of the whole machine of the diffuser alone is compared with some variations. For solving the problem of matching different components it is helpful to know parameters of the fluid flow in detail. This paper describes the improvement in matching obtained by changing the diffuser width.

TABLE 1. Design Parameters

Parameter	Description
Impeller	
d_2 = 400 mm	exit diameter
β_2 = 90°	exit angle
b_2 = 26.7 mm	exit width
Diffuser	
d_4 = 460 mm	inlet diameter
d_6 = 600 mm	exit diameter
b_4 = 24 or 21.6 mm	width
α_4 = 16.9°	inlet angle
α_6 = 26.9°	exit angle
z = 19	blade number

Experimental Set Up

The centrifugal compressor used for these investigations at the Institute of Turbomachinery at the University of Hannover has been used for numerous detailed flow investigations, initially with a vaneless diffuser /1/ and later on with several vaned diffusers with different vane-types /2, 3/. Fig. 1 shows a cross-section through the compressor.

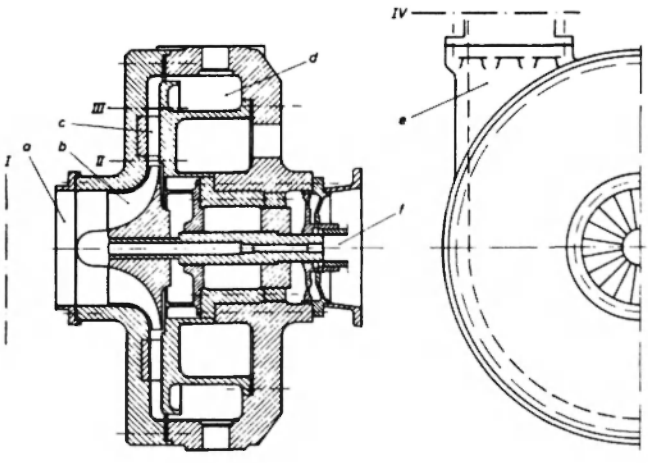

a inlet — *d collecting chamber*
b impeller — *e pressure pipe*
c diffuser — *f drive*
I - IV measuring sections

Fig. 1: Simplified sectional view of the compressor

The unshrouded impeller used for all these measurements has 28 radial-ending blades and an outer diameter of 400 mm. Further data can be found in Table 1. Measurements with an equal impeller are described by Krain in /4/.

A vaneless space of 15% of the impeller tip diameter allows a smoothing of the fluctuating impeller outlet flow before it reaches the leading edges of the 19 diffuser vanes. The design of the diffuser vanes is based on the flow measurements with the vaneless diffuser, which had a constant area of the flow channel at all radii.

The diffuser vane inlet angle was based on averaged flow angle measurements, well knowing that there is a variation in flow angle from hub to shroud. Because the geometry of the vaneless space had to be identical with the corresponding part of the vaneless diffuser, the width of the flow passage in the vaned part with parallel walls was specified by the selection of the inlet diameter of the vanes. This has been chosen to be at a radius ratio of λ = 1.15. The vanes end at a radius ratio of λ = 1.5. The inlet angle of the vane is 16.9° relative to the circumferential direction. It increases to the outlet by 10 degrees. In connection with this vaneless diffuser the impeller shows a wide flow range with little drop of efficiency at the lines of constant specific speed, as it is drawn in Fig. 2.

After the first cambered vane diffuser – consisting of a radial blade row shown in Fig. 3 – was compared with two wedge type diffusers /2/, it was decided that peak efficiency and pressure ratio of this type should be improved, especially for

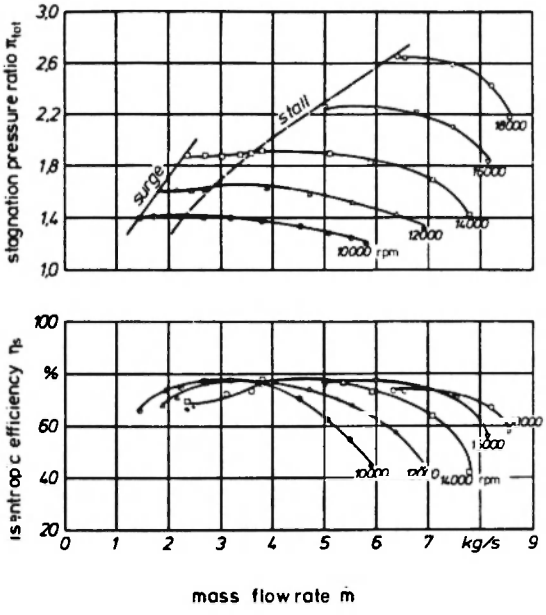

Fig. 2: Compressor map with vaneless diffuser.

high inlet Mach numbers corresponding to more than 20,000 rpm. Knowing that the variation of flow angle over the diffuser width did not match with the untwisted vane profile, there were two possible ways to go. One could design a vane taking in account this angular variation by a variation of inlet angle over the diffuser width as reported by Jansen /3/. Alternatively, one could try to influence the flow angle upstream of the diffuser vanes. The second idea was that a reduction of the passage width would block a region with extremely low flow angle at the shroud. Since the flow passing through this region represents only a small fraction of the entire through flow due to small flow angles, the flow through the narrow diffuser was expected to have a slightly larger flow angle. While Jansen's design leads to an increase of the choke mass flow at constant circumferential speed, the reduction of the passage width means a reduction in choke mass flow as well. This should be an additional way to increase peak efficiency, because the point of highest impeller efficiency is measured at lower mass flows.

The passage width reduction was accomplished by moving the diffuser hub wall as shown in Fig. 4. The stationary shroud for the impeller was remachined to allow the impeller to be moved forward. The impeller hub wall was even with the diffuser hub wall in both cases. In order to reach the original design mass flow of $\dot{m}_N$ = 8.59 kg/s a reduction of 14% passage width seemed to be reasonable, but the geometric conditions shown in Fig. 4 only

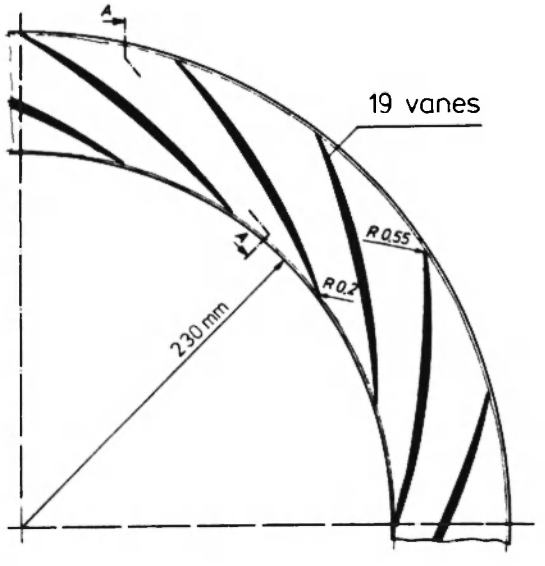

Fig. 3: Diffuser geometry.

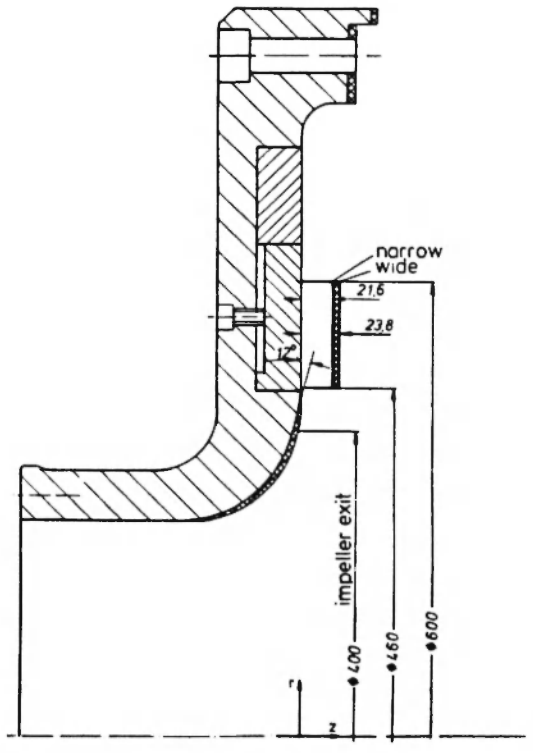

Fig. 4: Cross section of wide and narrow diffuser (in mm)

allowed a 10% reduction, because the impeller should be left unchanged. Intending to achieve a shroud contour without inflection, the diffuser cross section shows a straight line with an inclination of 12 degrees according to the angle of the shroud at impeller outlet. The connection to the parallel wall in the vaned part is described by a circular arc just ending at the tip of the vane. The diffuser vane geometry remained the same.

Investigations

First comparisons of the two diffusers described above can be made with the performance characteristics of the whole compressor stage by measuring the stagnation pressure and temperature in the equalizing chamber upstream of the stage and in the collecting tube. With the pressure ratio π_{tot} and the temperature ratio τ_{tot} the isentropic efficiency was calculated according to eq. (1):

$$\eta_s = \frac{\pi_{tot}^{(K-1)/K} - 1}{\tau_{tot} - 1} \qquad (1)$$

A calibration nozzle in the pressure tube allowed to determine the mass flow, which afterwards was reduced to reference conditions of p_0 = 0.981 bar and T_0 = 288.15 K. In order to get further informations of the diffuser performance, probe measurements upstream of the vanes at a radius ratio of λ = 1.1 and downstream of the vanes at a ratio of λ = 1.6 have been made. At four positions over the diffuser pitch and five positions over the width the stagnation pressure was measured with Kiel-probes while the flow angle was determined using a two hole Conrad-probe at the same positions.

A picture of the pressure recovery throughout the entire diffuser can be gained from the static pressure values at 81 positions at the shroud on 27 radii from λ = 1.0 to λ = 1.55 and another 19 positions at the hub between impeller exit and diffuser throat.

Two operation points near the surge line, one at 16,700 rpm, the other at 20,000 rpm have been chosen for the comparison of these measurements. At the lower shaft speed the mass flow rate is nearly identical in both diffusers. At 20,000 rpm the difference in mass flow rates, $\dot{m}$ = 8.20 kg/s for the wide one and 7.60 kg/s for the narrow one, corresponds to the difference in the choke flows.

Results

Compressor Maps

In the upper part of the compressor maps stagnation pressure ratio is drawn versus the reduced mass flow with lines of constant shaft speed n and constant isentropic efficiency η_s. In the lower part the efficiency is plotted versus mass flow. Fig. 5 shows the map of the wider diffuser, Fig. 6 the one of that with the reduced width.

The general character of both maps is similar but in Fig. 6 the lines of constant shaft speed are slightly shifted to lower mass flows. The maximum efficiency is still reached between 14,600 rpm and 16,700 rpm near surge but it has improved by nearly two points. The efficiency rise at high shaft speeds appears even more important. For example at 22,000 rpm near surge we have now measured η_s = 76% instead of η_s = 72%. At low shaft speeds there is no important change in efficiency. To get further information about the mechanism leading to these effects, detailed flow measurements have been made at several points of the map indicated by

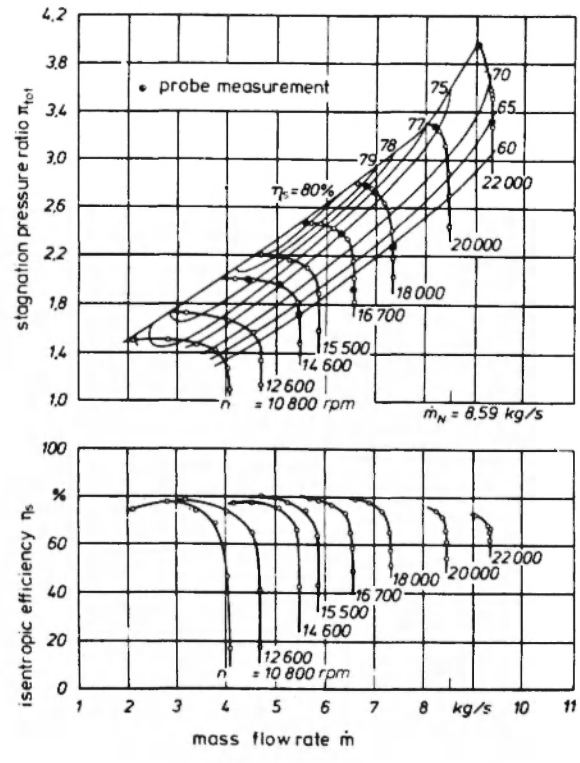

Fig. 5: Compressor map with wide diffuser.

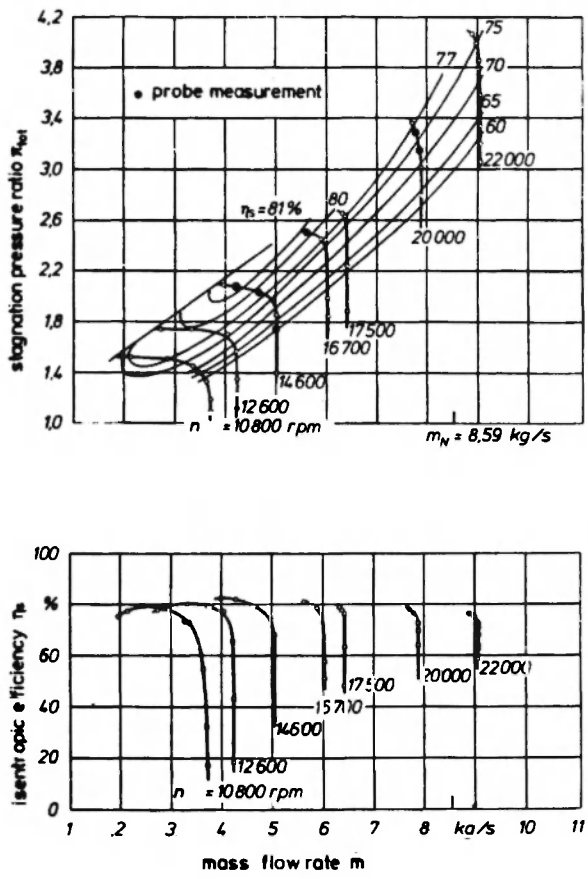

Fig. 6: Compressor map with narrow diffuser.

full circles. Some of these results will be discussed later on.

When comparing the two maps in Fig. 7 the effect of the reduction is most apparent in a shift of the choke lines to the left. At lower Mach numbers the difference between the choke flows is about 10%, which is proportional to the difference in passage width. Obviously, at 20,000 rpm and even more at 22,000 rpm other effects are taking place, leading to a flow reduction of 7% and 3% respectively. This, as well as the important rise in pressure recovery, may result in a change in boundary layer thickness at the throat. In terms of Runstadler's diffuser maps /5/ this means a change in throat blockage, because the length to width ratio and the area ratio remained the same and the aspect ratio is changed only slightly. As we can understand blockage partly as a function of leading edge incidence, further information should be taken out of the flow angle measurements.

Probe Measurements

For the comparison of the probe measurements the results at 20,000 rpm are chosen. Fig. 8 shows those with the wider diffuser. Upstream of the diffuser at $\lambda = 1.1$ the flow angle, measured relative to the circumferential direction, changes over a wide range with a nearly constant gradient from hub to shroud. There is also a change of flow angle over the pitch which indicates an upstream influence of the vanes. The stagnation pressure shows only minor differences over the pitch and a drop to the shroud. In passing through the diffuser channel, the gradient from hub to shroud disappears and the exit flow angle varies over the pitch only.

In Fig. 9 we see the result of the width reduction on flow angle at $\lambda = 1.1$. At the shroud the flow angle is not less than 15° and therefore the gradient is not so steep. Similarly, the stagnation pressure

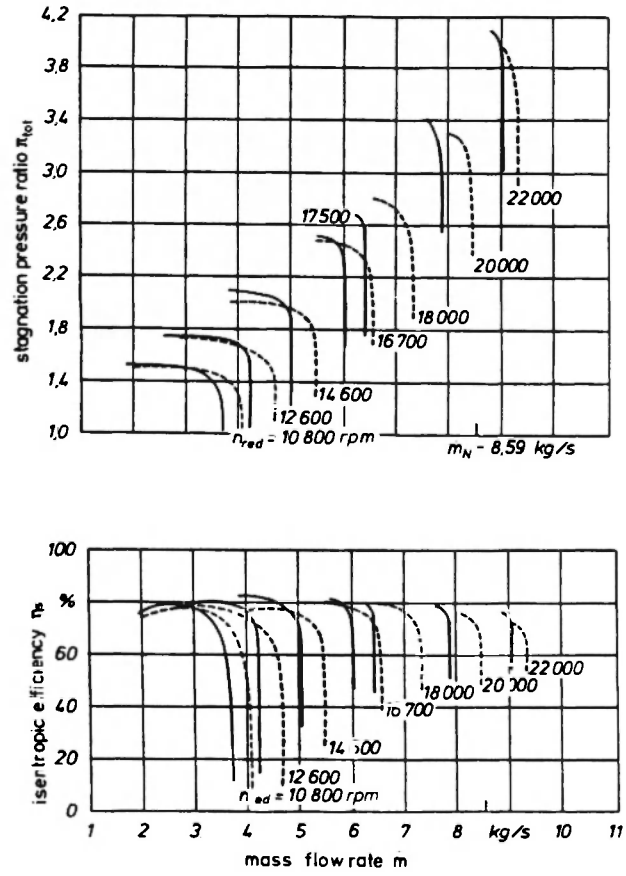

Fig. 7: Comparison of compressor maps
- - - wide diffuser
—— narrow diffuser

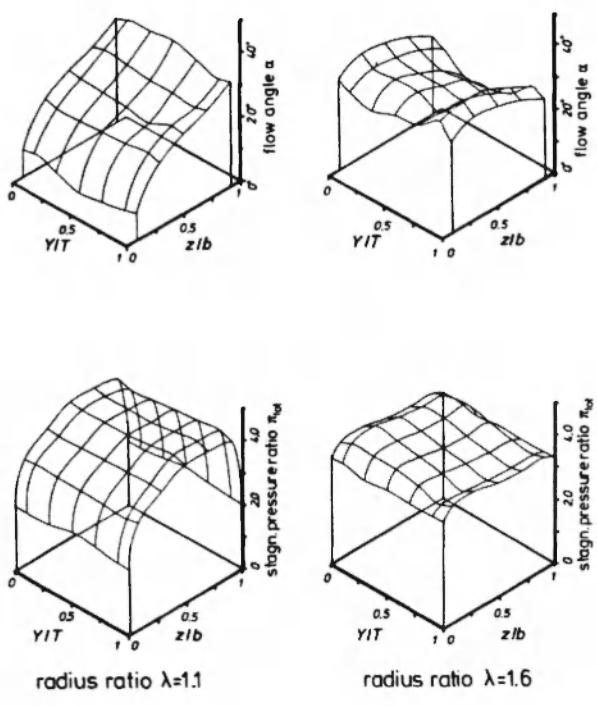

Fig. 8: Probe measurement in the wide diffuser versus pitch and width z/b
n = 20,000 rpm $\dot{m}$ = 8.2 kg/s

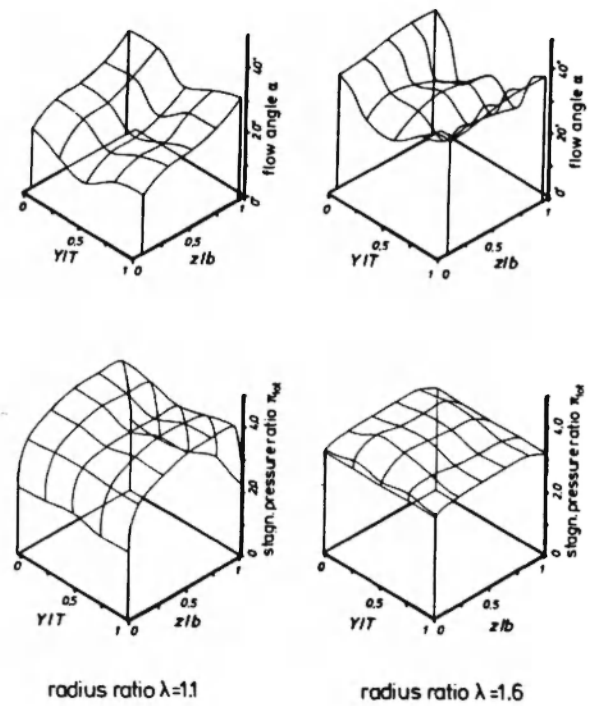

Fig. 9: Probe measurement in the narrow diffuser versus pitch and width z/b
n = 20,000 rpm $\dot{m}$ = 7.60 kg/s

is more or less constant with a decrease near the walls. Behind the diffuser the pressure is as uniform as it was with the wider diffuser vanes.

Static Pressure Distribution

Out of the static pressure measurements at hub and shroud isobars are calculated and plotted in the following figures.

Only values from the shroud were available for the wide diffuser, shown in Figs. 10 and 12. These results correspond to the rather low flow angles and the pressure recovery is very uniform. For the other diffuser the differences between hub and shroud can be seen in Figs. 11 and 13. At 16,700 rpm the pressure rise at the shroud in Fig. 11 is similar to that in Fig. 10, which is remarkable as we have the same mass flow in a smaller flow channel. At the hub there is a region of higher pressure in the inlet of the diffuser vanes, which is a reaction of the deceleration causing the change in flow direction between the higher flow angle at the hub and the vane channel.

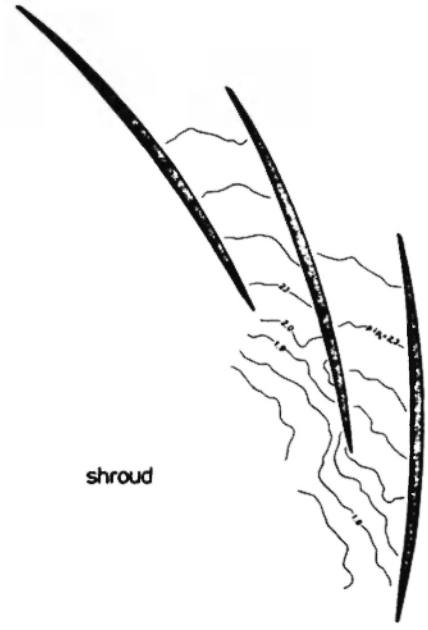

Fig. 10: Static pressure distribution in the wide diffuse
n = 16,700 rpm $\dot{m}$ = 5.66 kg/s

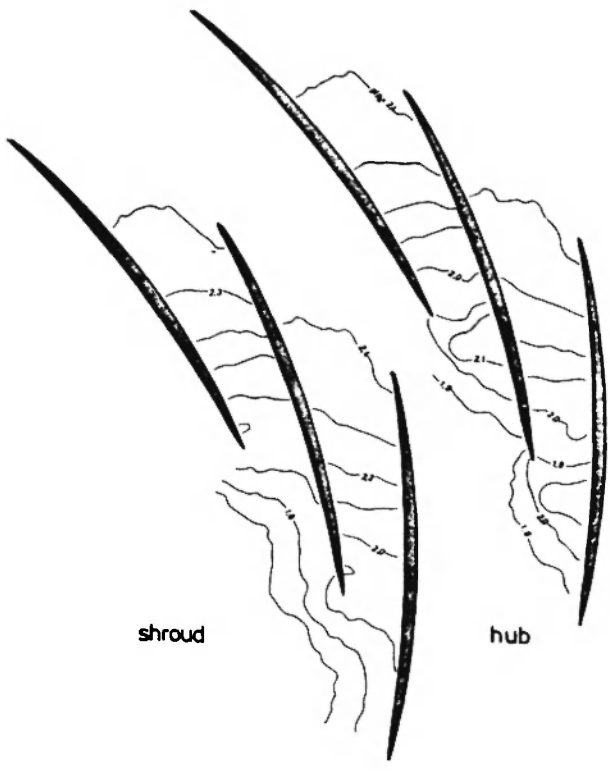

Fig. 11: Static pressure distribution in the narrow diffuser
n = 16,700 rpm $\dot{m}$ = 5.65 kg/s

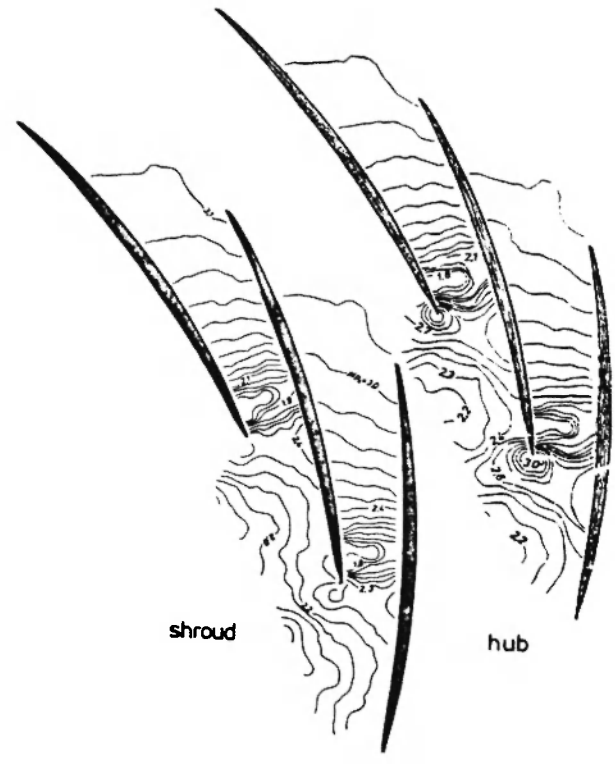

Fig. 13: Static pressure distribution in the narrow diffuser
n = 20,000 rpm $\dot{m}$ = 7.60 kg/s

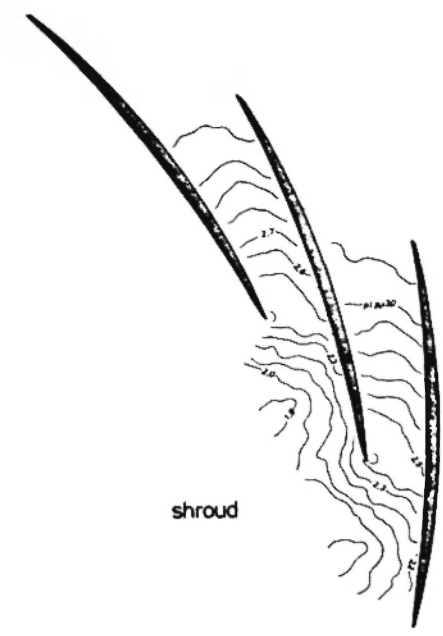

Fig. 12: Static pressure distribution in the wide diffuser
n = 20,000 rpm $\dot{m}$ = 8.20 kg/s

In Fig. 13 these pressure gradients in the inlet are even bigger and indicate a higher impeller exit Mach-number as well as a greater margin to surge flow. Even at the shroud there is a zone of acceleration near the throat. The differences between hub and shroud disappear near the throat. Therefore in front of it there are regions where the angle differences over the width of the vaneless and semi-vaneless space are equalized leading to three dimensional pressure distributions.

Conclusions

One way of improving the matching of an untwisted guide vane in the diffuser of centrifugal compressors, which have a considerable variation of the flow angle over the passage width at the impeller outlet, is the reduction of the width of the vaneless space upstream to the diffuser vanes. Because the circumferential area at the tip of the vanes is smaller than at impeller outlet this in general means an acceleration of flow velocity, which should

have disadvantages for the pressure recovery. However, it could be demonstrated, that especially at high shaft speeds this reduction has an equalizing effect on the flow angle, which leads to improved flow conditions at the entrance to the vaned part. The variation of the flow angle between hub and shroud reaching about 30° at some operation points is reduced to about 10° as a consequence of the width reduction. A comparison of the averaged flow values downstream of the impeller does not indicate important changes to the impeller flow characteristic. At least for lower shaft speeds up to 16,700 rpm diffuser flow seems to have little influence on the impeller flow. The effects at high shaft speeds are the subject of further investigations.

The shift of the surge line to the right in Fig. 7 had been expected to be as big as that of the choke line. Unfortunately, this could not be reached. But among those diffusers measured on this test rig, the narrow one has the smallest difference in surge flow to that of the compressor with vaneless diffuser.

An improvement of the tested diffusers seems to be possible by using twisted vanes in the narrow diffuser. The smoothing of the flow angle upstream of the diffuser leads to a geometry of the twisted vanes that would be easier to design and manufacture.

Acknowledgements

The subject reported in this paper has been investigated in connection with the "Sonderforschungsbereich 61: Stroemungsprobleme in der Energieumwandlung" at the University of Hannover in the Institute for Turbomachinery. The financial support of the Deutsche Forschungsgemeinschaft is gratefully acknowledged.

The authors wish to express their appreciation for the efforts of Mr. P. Tanneberg who prepared and operated the test rig.

References

1. K. Bammert and M. Rautenberg, "On the Energy Transfer in Centrifugal Compressors", ASME Paper No. 74–GT–121, 1974.
2. K. Bammert, M. Jansen, P. Knapp and W. Wittekind, "Stroemungsuntersuchungen an beschaufelten Diffusoren fuer Radialverdichter", Konstruktion 28, pp. 313–319, 1976.
3. M. Jansen and M. Rautenberg, "Design and Investigations of a Three Dimensional Twisted Diffuser for Centrifugal Compressors", ASME Paper No. 82–GT–102, 1982.
4. H. Krain, "A Study of Centrifugal Impeller and Diffuser Flow", ASME Paper No. 81–GT–9, 1981.
5. P.W. Runstadler, "Diffuser Data Block", Creare TN–182, 1975.